

Unitary description of the black hole by prime numbers

M. Bousder^{1*}

¹LPHE-MS Laboratory, Department of physics,
Faculty of Science, Mohammed V University in Rabat, Rabat, Morocco

November 9, 2021

Abstract

In this paper, we study the thermofield double states of doubly-holographic gravity in two copies of the horizons. We show that the asymptotically AdS spacetimes describe an entangled states of a pair of CFTs based on the Farey sequence. We propose a new technique to geometrize the black hole horizon. Our protocol is based on the so-called Farey diagram. We construct states and entropies to describe the unit cells on the horizon. As a result, we have proved that the quantum states on the horizon are encoded by prime numbers. Therefore, we found that the entropy of the code space and area law are writtens in logarithmic form of the prime numbers. We show that the number of connected components of the Farey sequence can build the Fermi–Dirac distribution. To solve the information paradox problem, we find that the Hawking radiation follows geodesic of the Farey diagram, then he turns around and falls on the horizon. Our aim is to show that there is appearance of several Page times, because of discontinuous emission of these radiations. Finally, we mention the possibility to describe the quantum Hall effect by using the Farey diagram. In this paper, we find a link between quantum information and the theory of numbers passing through geometry.

Keywords: Thermofield double, Black hole, Information paradox, Entanglement entropy.

1 Introduction

(i) *Background.*

In recent breakthrough works, the loss of information during the evaporation of black

*mostafa.bousder@um5.ac.ma

holes is an open problem [1]. Many proposals were suggested to resolve the information paradox. In a lines of the introduction we discuss the attempts to solve this problem:

- In *AdS/CFT* [2], the $d+1$ -dimensional quantum gravity (AdS) is dual to d -dimensional conformal field theory (CFT) which lives on the asymptotic boundary of space-time. The *AdS/CFT* correspondence shows that information can escape from a black hole. The unitarity of the CFT implies the information reservation, so, the black hole evaporation process is expected to be unitary [3]. In this case, the evaporation of the black hole has a dual unitary description in the CFT.

- The so-called Page curve as a function of time describes the unitary process of black hole evaporation [4, 5]. In this curve, the entropy increases until the Page time, then it begins to decrease. In Jackiw-Teitelboim (JT) gravity in AdS_2 , the Page curve was reproduced explicitly without assuming the unitarity. At the Page time, the entanglement entropy in the black hole transition marks a change between initial and final states. Before the transition, there is a simple spatial division between the radiation and the degrees of freedom of the black holes. After this transition, the interior region of the black hole covered by the island structure [6]. In [7], the entanglement wedge reconstruction occurs in the island, i.e. inside the black hole "interior".

- In [8], the Page curve is reproduced according to the Ryu-Takayanagi (RT) formula for the von Neumann entropy of radiation, which was inspired by the quantum extremal surface formula (QES) for the holographic entanglement entropy. The entanglement entropy (EE) of a boundary region is given by the area of RT surfaces, corresponding to the bulk minimal surface. The thread prescription which is equivalent to the quantum extremal surface (QES) prescription [9, 10].

- The ER = EPR [11] has given a new perspective on the gauge/gravity correspondence. Under this paradigm, a pair of entangled black holes are joined by an Einstein-Rosen (ER) bridge. This suggests that there is a relation between quantum entanglement and geometric spatial.

- The construction of multi-boundary or wormholes was applied in the framework of the End-of-the-World (EOW) brane model [12] in three dimensions and without quantum fields.

- Recent work has focused on the issue of the thermofield double (TFD) states is a central ingredient. The connection between boundary information-theoretic quantities and bulk areas has been extended to a conjectured [13]. In parallel, there have also been numerous proposals to directly modeling the black hole (BH) evaporation and calculations of the entanglement entropy [14].

- In [15], the black hole AdS geometry is coupled to a bath which absorbs the black hole radiation, also the Page curve is characterized by the unitary black hole evaporation.

(ii) *Goal and strategy.*

In this work, we present a preparation scheme for Farey sequence that can be implemented on a CFT_d on the boundary asymptotically AdS_{d+1} boundary of the dual gravity theory. Our first goal then is to figure out what the relation is between the TFD state the geometry of the region near horizon and. Our second goal is to determine the black hole statistic by using the TFD states. In this basis, we imagine a temperature at the horizon tends to ∞ . Then write the states $|TFD\rangle$ as a function of the states $|TFD(\beta = 0)\rangle$. This new technique will allow us to find another path to determine both the geometry, the state encoding and the statistics of the black hole. By studying the the number of BH states, we can understand that the BH undergoes the Fermi–Dirac particle-energy statistics.

To study the entanglement entropy between the BH radiation and the quantum state associated to the remaining BH in the framework of the Page curve. We propose a new description which begins with the study of TFD states in the horizon. Then we propose a particular operator which can destroy the entanglement at the infinite temperature, and we write TFD states in terms of this operator. We assume that the destruction of the entanglement is done in the time of Page. Our aim is to geometrize the AdS background of the BH in the presence of entangled states. When we remove the entanglement by the operator, then we build the entanglement by the results of calculations, we find the AdS geometry dual to CFT of the entangled states. This geometry allows to see the entanglement as a geodesic in the background. Our results show that there is not a loss of Hawking radiations in space-time, but the radiations follow a special geodesic generated by the Farey diagram lines.

(iii) *Organization.*

The paper is organised as follows. In Section 2 we introduce and review the TFD with an operator that removes entanglement for an infinite temperature ($T \rightarrow \infty$). Then in Section 3 we discuss the AdS background geometry by the description of the CFT states at $T \rightarrow \infty$, from the point of view of the Farey diagram. Following that, in Section 4 we build microstates of unitary description in Farey diagram (AdS geometry), and we find a connection between multi-boundary and microstates. In Section 5 we find that the Fermi-Dirac statistics governs unitary processes of the system. Using the black hole first law of thermodynamics in Section 6 we find a quantum description of the CFT states by the quantum hall effect. In Section 7 we present some conclusions and outlook.

2 Left and right horizons in CFT

(i) *Motivation*

Let $H = H_L \otimes H_R$ be the Hilbert space of the full *CFT* and $|u\rangle$ denote the quantum state of a system with N particles. Hamiltonian evolution is generated by $H_{TFD} = 1_L \otimes H_R + H_L \otimes 1_R$. Let us define the thermofield double (TFD) state as a particular entangled state [16, 17]:

$$|TFD\rangle = \frac{1}{\sqrt{Z(\beta)}} \sum_j e^{-\beta E_j/2} |u_j\rangle_L \otimes |\bar{u}_j\rangle_R, \quad (2.1)$$

where Z is the partition function of the CFT at temperature $T = \beta^{-1}$ and $e^{-\beta E_j/2}/\sqrt{Z(\beta)}$ is a normalization factor such that ${}_k \langle TFD | TFD \rangle_k = 1$. The TFD state was suggested outside of the black holes. In this last equation, we consider t as a parameter labeling time-dependent TFD state at a common instant $|TFD(t)\rangle = e^{it(H_L+H_R)} |TFD\rangle$. In each of these states at time t , there exists a projection operator $P_t = |TFD(t)\rangle \langle TFD(t)|$. According to [11], two entangled states with different values of t are linked by the forward time evolution on the two sides of *CFT*. Note that the projection operator is expressed in terms of t . $|u_j\rangle_{LR}$ defined in the microscopic UV-complete theories, they create *CFT* states with energy [18]. By tracing out the exterior states in one horizon we obtain the density matrix. The mixed state given by the incoherent sum over all generalized TFD states $\rho_{TMD} = (1/N) \sum_j |TFD\rangle_j {}_j \langle TFD|$ call the the thermo-mixed double, where N the total number of basis states. The thermal density matrix as arising from entanglement. The corresponding bulk geometry of the wormhole is formed by $tr(\rho_{TMD}^2) = \sum_j e^{-2\beta E_j}/Z^2$, where $Z = \sum_j e^{-\beta E_j}$ is partition function, with the square number 2 corresponds to the two horizons.

We consider the TFD of dual to the left and right sides of the geometry by two copies of the horizons \mathcal{H}_L (left horizon) and \mathcal{H}_R (right horizon) in CFT. The eigenstate $|u_j\rangle_L$ (or $|\bar{u}_j\rangle_R$) of the CFT_L (or CFT_R) correspondes to the degrees of freedom in \mathcal{H}_L (or \mathcal{H}_R). In the context of holographic gravity, the two sides of *CFT* are connected by a wormhole, or ER bridge, according to the *TFD* states Eq.(2.1). The *TFD* is a maximally entangled state, which represents the formal purification of the thermal mixed state of a one horizon (\mathcal{H}_L or \mathcal{H}_R) [19], with the reduced density matrix within *AdS/CFT* via the Ryu-Takayanagi formula [8].

(ii) *Strategy*

To study TFD states at the time of entanglement removal at an infinite temperature ($\beta = 0$) in the horizon. We start by define an entangled state which is expressed as

$$|\psi\rangle = |TFD(\beta = 0)\rangle_{LR} + |TFD(\beta = 0)\rangle_{RL} \in H. \quad (2.2)$$

At this point, the entangled state can be decomposed into a LR and RL part as follows

$$|\psi\rangle = \frac{1}{\sqrt{Z(\beta)}} \left(\sum_{j=1}^{N_-} |u_j\rangle_L \otimes |\bar{u}_j\rangle_R + \sum_{k=1}^{N_+} |\bar{u}_k\rangle_R \otimes |u_k\rangle_L \right), \quad (2.3)$$

Here, N denotes the number of the quantum state, where $N = N_- + N_+$, with the number N_- and N_+ of copies of the states $|u\rangle$ and $|\bar{u}\rangle$, respectively, and $|u_j\rangle \neq |u_{j+1}\rangle$. We define an unitary operator \mathcal{W} which verifies

$$\begin{aligned} \mathcal{W}|u_j\rangle_L &= (-1)^{j-1} |u\rangle_L, \\ \mathcal{W}|\bar{u}_j\rangle_R &= (-1)^{j-1} |\bar{u}\rangle_R, \\ \mathcal{W}^2 &= 1, \end{aligned} \quad (2.4)$$

the aim of this operator is to remove the interaction between states near horizon at $\beta = 0$. We find

$$\mathcal{W}|\psi\rangle \sim \sum_{j=1}^{N_-} (-1)^{j-1} |u\rangle |\bar{u}\rangle + \sum_{k=1}^{N_+} (-1)^{k-1} |\bar{u}\rangle |u\rangle, \quad (2.5)$$

which leads to

If N_- is even and N_+ is even, one obtain $\mathcal{W}|\psi\rangle = 0$.

If N_- is even and N_+ is odd, one get the pure state $\mathcal{W}|\psi\rangle \sim |\bar{u}\rangle |u\rangle$.

If N_- is odd and N_+ is even, one get the pure state $\mathcal{W}|\psi\rangle \sim |u\rangle |\bar{u}\rangle$.

If N_- is odd and N_+ is odd, one get the entangled state $\mathcal{W}|\psi\rangle \sim |u\rangle |\bar{u}\rangle + |\bar{u}\rangle |u\rangle$.

If N is infinite, one get the entangled state $\mathcal{W}|\psi\rangle_\infty \sim \frac{1}{2} (|u\rangle |\bar{u}\rangle + |\bar{u}\rangle |u\rangle)$, ($\zeta(0) = 1/2$, the analytic continuation of the Riemann zeta function).

(iii) Results

We can map initial state $|\bar{u}\rangle |u\rangle$ and final state $|u\rangle |\bar{u}\rangle$ in the CFT, then we can compute the entanglement between the two states in the CFT. This procedure can represent by the following quantification. The states $|0\rangle$ and $|\bar{0}\rangle$ are the Rindler vacuum states in the two exterior region horizons in the right and left horizons, respectively. The state $|0\rangle |\bar{0}\rangle$ is the outside horizons vacuum states.

The state $\mathcal{W}|\psi\rangle$ is transformed to

$$\mathcal{W}|\psi\rangle \sim \alpha |u\rangle |\bar{u}\rangle + \beta |\bar{u}\rangle |u\rangle, \quad (2.6)$$

with

$$(\alpha, \beta) = \begin{cases} (0, 0) \\ (0, 1) \\ (1, 0) \\ (1/2, 1/2) \\ (1, 1) \end{cases}, \quad (2.7)$$

such that $(\alpha, \beta) \geq (0, 0)$ are quantum numbers. The results of this section suggest that $|TFD\rangle = \mathcal{W} \left(\sum_j \sqrt{p_j} e^{i\omega_j} |\psi\rangle_j \right)$. We can reexpress the TFD states in terms of the $(\beta = 0)$ modes as

$$|TFD\rangle = \frac{1}{\sqrt{Z(\beta)}} \sum_{j=1}^N e^{-\beta E_j/2} \mathcal{W} (|TFD_j(\beta = 0)\rangle_{LR} + |TFD_j(\beta = 0)\rangle_{RL}). \quad (2.8)$$

As previously mentioned, we adopt the states $|TFD(\beta = 0)\rangle$ to evaluate the geometric approach of two copies of the horizons in the holographic CFT. The volume of this geometry increases in time according to the number of degrees of freedom of the boundary theory. Note that we can rewrite the state $|\psi\rangle$ as

$$|\psi\rangle \sim N_+ |u\rangle |\bar{u}\rangle + N_- |\bar{u}\rangle |u\rangle. \quad (2.9)$$

For entangled states, the left and right systems are identical ($N_- = N_+ = N/2$), the state $|\psi\rangle$ can be represented as $|\psi\rangle \sim \frac{N}{2} (|u\rangle |\bar{u}\rangle + |\bar{u}\rangle |u\rangle)$. Comparing Eq.(2.3) to Eq.(2.6), we conclude that

$$|u\bar{u}\rangle = \frac{N_- - \beta}{\alpha - N_+} |\bar{u}u\rangle. \quad (2.10)$$

where $|u\bar{u}\rangle = |u\rangle |\bar{u}\rangle$. Using the normalization: $\langle u\bar{u} | u\bar{u} \rangle = 1$, we notice that $\alpha + \beta = N$ or $\alpha - \beta = N_+ - N_-$. Then, by applying this observation, we obtain

$$\begin{aligned} |u\bar{u}\rangle &= + |\bar{u}u\rangle \text{ for } \alpha + \beta = N, \\ |u\bar{u}\rangle &= - |\bar{u}u\rangle \text{ for } \alpha - \beta = N_+ - N_-. \end{aligned} \quad (2.11)$$

Since the Eq.(2.7) satisfy $\alpha + \beta = \{0, 1, 2\}$ and $\alpha - \beta = \{-1, 0, 1\}$, we can reexpress the generator in terms of the N modes as

$$\begin{aligned} |u\bar{u}\rangle &= + |\bar{u}u\rangle \text{ for } N = \{1, 2\}, \\ |u\bar{u}\rangle &= - |\bar{u}u\rangle \text{ for } N \geq 2. \end{aligned} \quad (2.12)$$

These two relationships above, implies that the state $\mathcal{W}|\psi\rangle$ is not an entangled state

$$|\psi\rangle \xrightarrow{\text{entanglement removal}} \mathcal{W}|\psi\rangle. \quad (2.13)$$

The operator \mathcal{W} allows the system to be transferred to another state. In this case we suppose that before the Page time the black hole exists in the state $\mathcal{W}|\psi\rangle$, after this time, the outgoing radiation and the quantum state associated to the remaining black hole are entangled according to the state $|\psi\rangle$.

$$\mathcal{W}|\psi\rangle \xrightarrow{\text{after Page time}} |\psi\rangle.$$

To describe the Majorana states we can choose $N = 2$ for the first case Eq.(2.12). The change of sign (+) to (-) in $N = 2$, lead to additional degeneracy.

Now, we consider $N_+ = N_- = N/2$. The coherent states can be expressed in terms of Fock states in the standard way as

$$|\psi\rangle = \frac{1}{\sqrt{Z(\beta)}} \left[\sum_{j=1}^{N_-} e^{-\beta E_j/2} |u_j\rangle_L \otimes e^{+\beta E_j/2} |\bar{u}_j\rangle_R + \sum_{k=1}^{N_+} e^{+\beta E_k/2} |\bar{u}_k\rangle_R \otimes e^{-\beta E_k/2} |u_k\rangle_L \right]. \quad (2.14)$$

We use the transformation

$$\sqrt{2}e^{+\beta E_j/2} |\bar{u}_j\rangle_R \longrightarrow |\bar{u}_j^*\rangle_R, \quad |u_k\rangle_L \longrightarrow |u_k^*\rangle_L \quad (2.15)$$

then, the evolution of the horizon geometry is described by the following entangled state

$$|\psi(t)\rangle = \frac{1}{\sqrt{2}} (|TFD^*(t)\rangle_{LR} + |TFD^*(t)\rangle_{RL}), \quad (2.16)$$

where $|TFD^*(t)\rangle_{LR}$ is the evolution of the TFD state in the horizon from L to R at time t . If we compare Eq.(2.16) with Eq.(2.2), we notice that in the horizon at $\beta = 0$, there is still an evolution of the system over time. Indeed, the temperature is infinite only in certain time, but the equivalence between Eqs.(2.2,2.16), shows that the temperature is infinite in all time: $\forall t, |TFD(\beta = 0)\rangle_{LR} \sim |TFD^*(t)\rangle_{LR}$. This shows that there is always a production of the Hawking radiation. Therefore, there is always an entanglement between these radiations and the remaining hole. This may be due to several effects, but the most realistic effect is that the radiation comes out of the black hole, after a certain time it follows spetial geodesic so that they go back and fall on the BH horizon. The objective in the next section is to determine this geodesic.

3 Farey diagram of the AdS background

To determine the geodesic of the Hawking radiation, we try to find a geometric that is hidden behind the evolution of states $\mathcal{W}|\psi\rangle$ and $|\psi\rangle$. As illustrated above, we also wish to express the state $|u\bar{u}\rangle$ in terms of the number of states acting on the state $|\bar{u}u\rangle$. Let us start by considering the three cases $(\alpha, \beta) = \{(0, 0); (0, 1); (1, 0)\}$ Eqs.(2.6,2.9). Then, the corresponding states generated by

$$|u\bar{u}\rangle_{\beta=0} = \frac{N_-}{\alpha - N_+} |\bar{u}u\rangle, \quad |u\bar{u}\rangle_{\alpha=0} = \frac{\beta - N_-}{N_+} |u\bar{u}\rangle. \quad (3.1)$$

A new value of α and β is in principle determined by the normalization: $\langle u\bar{u} | u\bar{u} \rangle = 1$, one could take

$$\alpha = \{(N_+ - N_-); N\}_{\beta=0}, \quad \beta = \{(N_- - N_+); N\}_{\alpha=0}. \quad (3.2)$$

Here, we have $N \neq 0$. To check the conditions Eqs.(2.7,3.2), we distinguish between two cases:

(i) For the two cases: $\alpha = N_+ - N_-$ or $\beta = N_- - N_+$, the number of states are $N > 1$. (ii) For $\alpha = N$ or $\beta = N$, we have obtained only $\alpha = \beta = N = 1$, i.e. only one state in the system. When $N = N_+ - N_-$, one could take one degenerate solution corresponding to $N_- = 0$, which agrees with the violation of CP symmetry between matter and antimatter [20]. Therefore, the black hole behaves under the normalizable states as Schwarzschild or extremal black hole. Obviously, this distinction between the cases of α and β , can simplify the equation Eq.(3.1) as

$$\begin{aligned} |u\bar{u}\rangle &= |\bar{u}u\rangle \quad \text{for } N = 1, \\ |u\bar{u}\rangle &= -|\bar{u}u\rangle \quad \text{for } N > 1. \end{aligned} \quad (3.3)$$

Then, the corresponding states generated by

$$|u\bar{u}\rangle = (-1)^{1+\delta_N} |\bar{u}u\rangle, \quad (3.4)$$

where $\delta_N (N = 1) = 1$ and $\delta_N (N \succ 1) = 0$. Both cases Eq.(3.1) give the same result above. These states are invariant under the transformation $\delta_N \rightarrow -\delta_N$. Therefore, the state $|u\bar{u}\rangle$ is formulated in terms of the state $|\bar{u}u\rangle$, the main reason is that this relation gives an aspect in of a wormhole between the two states. It was explicitly confirmed by ER bridges from ER = EPR [21]. This result is equivalent to the sum of the Möbius function $\mu(N)$ over N

$$\delta_N = \sum_{k|N} \mu(k) = \begin{cases} 1 & \text{if } N = 1 \\ 0 & \text{if } N \succ 1 \end{cases}, \quad (3.5)$$

where

$$\mu(N) = \sum_{\substack{1 \leq k \leq N \\ \gcd(k, N) = 1}} e^{2\pi i \frac{k}{N}}. \quad (3.6)$$

This algebraic proof shows that the connection between the two horizons \mathcal{H}_L and \mathcal{H}_R is realised the Möbius function. Thus allowing to the Mertens function:

$$\mathcal{M}_N = \sum_{k=1}^N \mu(k) = -1 + \sum_{n \in \mathcal{F}_N} e^{2\pi i n}, \quad (3.7)$$

where \mathcal{F}_N denotes the Farey sequence of order N [22]. The quantum number α Eq.(2.7), consists of a contribution from the Farey sequence. The number α can be encoded into $\mathcal{F}_2 = \{\frac{0}{1}, \frac{1}{2}, \frac{1}{1}\}$. Let us consider the fraction $\frac{a}{b} \in \mathcal{F}_N$, there is a Ford circle $\mathcal{C}[\frac{a}{b}]$ with the radius $1/(2b^2)$ and centre at $(\frac{a}{b}, \frac{1}{2b^2})$. The Farey diagram describes a geometry near the AdS horizon. The Farey diagram \mathcal{F}_N of order $N \rightarrow \infty$ is given by

$$\mathcal{F}_\infty = \left\{ \frac{a}{b} : (a, b) \in \mathbb{Z}, \gcd(a, b) = 1 \right\} \cup \left\{ \frac{1}{0} \right\}. \quad (3.8)$$

The graph \mathcal{F}_N is associate to a closed surface of genus. This represents that the edges indicate geometric intersection number equal to N [23]. In fact, we hcan also study the possible symmetries of the Farey diagram using 2×2 matrices correspond to linear transformations of the plane from linear algebra, see Fig.1.

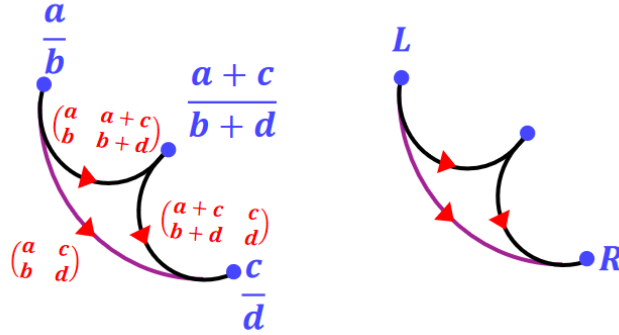


Figure 1: To go from \mathcal{H}_L to \mathcal{H}_R , we can use the 2×2 matrices correspond to linear transformations, which are formed by Farey sequence.

Each such vertices of $\frac{a}{b} \in \mathcal{F}_N$ has two primitive elements (a, b) and $(-a, -b)$. This makes it possible that a/b and $(-a)/(-b)$ are two different descriptions of the same state. In Fig.2 we give an example of Farey diagram.

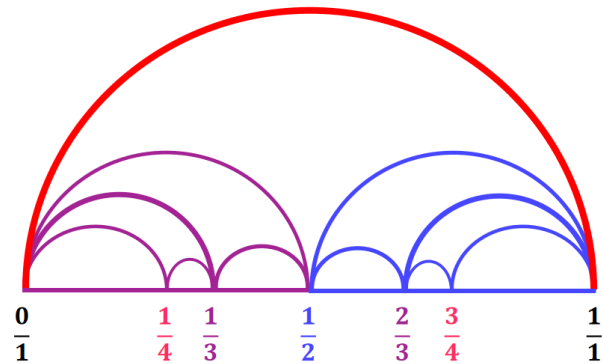


Figure 2: The Farey diagram \mathcal{F}_4 represented with circular arcs by the fraction values.

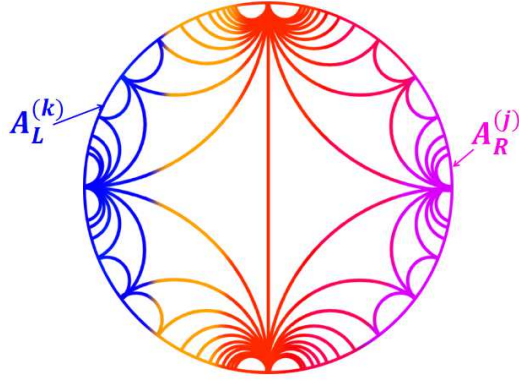


Figure 3: The bulk minimal surfaces of the subregions of \mathcal{A}_L and \mathcal{A}_R . In the surface, we see the presence of semi-circles, which means, in the horizon there is the presence of edge states. This corresponds to the quantum hall effect.

The Farey sequences of order n in $CFT = \mathcal{A}_L \cup \mathcal{A}_R$ circle encode an information contained in a set of coefficients $\frac{a}{b}$. This result can be extended to include subregions Fig.3: $\mathcal{A}_{L \text{ or } R}^{(n)} \subset \mathcal{A}_{L \text{ or } R}^{(n-1)} \subset \dots \subset \mathcal{A}_{L \text{ or } R}^{(1)} \subset \text{ou}\mathcal{A}_{L \text{ or } R}$. Following this procedure we obtained the n -point correlation function corresponding to the fraction points of the Farey diagram. Later, we will see a new description of n -point correlation function, like q cell is characterized by q -bit code. Each curve in Fig.3, represents a geodesic connection entanglement wedge between two horizon points. This geodesic represents the quantum states of black hole interior and only the description of the black hole entropy. On the other hand, there remains the geometric description of the exterior region of the black hole and the Hawking radiation. If we complete the circles in the border of the Farey diagram, we will construct the geodesics of the exterior region

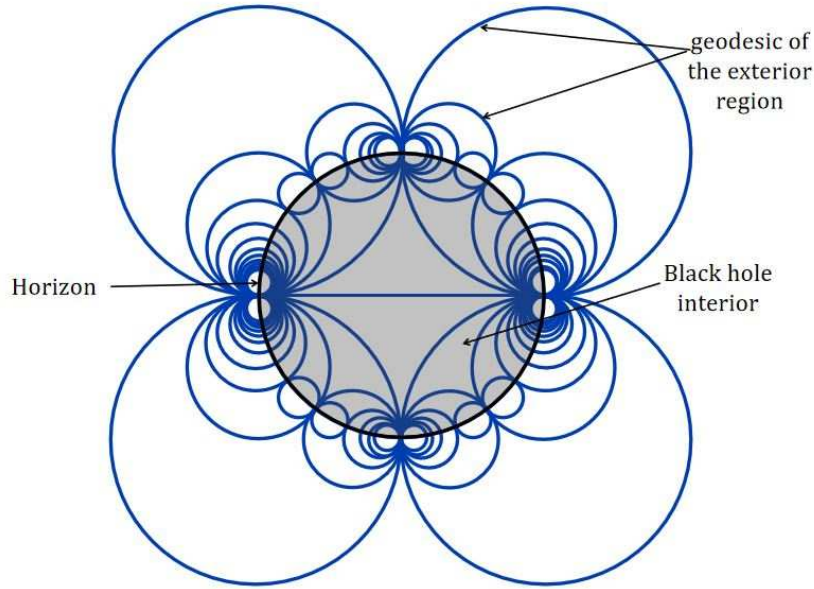


Figure 4: To obtain Farey diagram, we employ the Ford circle [34]. The diagram also makes it very clear that there the event horizons in Ford space. The Ford circle are equivalent to the cyclotron orbit of the edge states in the near horizon region.

The geodesic of Farey diagram in the exterior region is in a good agreement with the bath coupled to AdS black hole [15], which absorbs the radiation from the black hole. From Fig.4, we identify the curves in the exterior region as the geodesic of the trajectory of the Hawking radiation. The permanent creation of radiation Eq.(2.16), is due to the rotation of radiation in the same circles over time. According to this geodesic, the radiation does not fall into the black hole due to gravity but because of the special geodesic of the Farey diagram. The origin of the radiation geodesics, is the projection of evolution of TFD states in AdS, since AdS is the dual of CFT. So, the CFT states correspond to the AdS geodesics. The interaction between the horizon and the Hawking radiation create coding cells, which can be identified by $\mathcal{A}_{L \text{ or } R}^{(n)}$. To complete this geometrical description, one must treat this geodesic according to the unitary description [24].

4 Unitary prime description of AdS geometry

The Farey diagram of the AdS geometry is a construction of multi-boundary connection between microstates. The Multi-boundary can be obtained by evaluating the Euclidean CFT path integral on a cut Riemann surface [31]. The connection between the circles in the Farey diagram, represent the encoding of information. The number of connected

components of \mathcal{F}_N is constructed as follows

$$N_{con}(\mathcal{F}_N) = \begin{cases} p^{q-1}(p+1) & \text{if } N = p^q \\ \infty & \text{otherwise.} \end{cases}, \quad (4.1)$$

where p is a prime and q is a positive integer. When N is not a prime power, the number of connected components is infinite. We are interested by the solution where $N = p^q$. This indicates that the convergence to the large N limit is fast. The exponential degeneracy of the field theory vacuum states, indicated by the number

$$N_{vac} = e^{q \log p}, \quad (4.2)$$

which corresponds to the number of vacuum states in [24] if the entropy of a vacuum is $S_{vac} = ql_P^2 \log p$, where $l_P = \sqrt{\hbar G/c^3}$ is the Planck length. Therefore, the logarithm of the prime number of independent quantum states describes the boundary structure of the black hole. This number is also equivalent to the number of black hole states consistent with the boundary structure described above. We consider a lattice system in the horizon, each q cell is describe by a Farey fraction $\frac{a}{b}$. This implies that S_{vac} is obtained only after we include a prime number p . Also N_{vac} represents the number of possible independent ways to describe CFT on a fixed classical spacetime background (semi-classical physics). Let us elaborate the entropy of the near horizon region in a similar way to the Bekenstein-Hawking formula. The black hole first law of thermodynamics reads $S_{BH} = \int dM/T$. The validity of the generalized second law of thermodynamics suggests that it is given by the exponential of the Bekenstein-Hawking entropy $S_{BH} = A/4$ [24], where A is the area of the horizon. More precisely, the black hole horizon is encoded on each q cell by the prime number of states

$$p = \exp(A/4ql_P^2). \quad (4.3)$$

According to [24], the term $\exp(A/4ql_P^2)$ is the the total number of black hole vacuum states $|\psi_q\rangle$ for a fixed mass, where $q = 1, 2, \dots, p$. The entropy S_{BH} will be the encoding of p for p cell and we write that

$$S_{BH} = pl_P^2 \log p. \quad (4.4)$$

Therefore, the prime numbers p are always the total number of states of a black hole. In this view, the state $|u\bar{u}\rangle$ gives the unit cell with area l_P^2 . Sometimes the existence of the connected components of \mathcal{F}_N Eq.(4.1) is presented as a consequence of the area law. This shows that \mathcal{F}_N diagram is a new geometrization of black hole. In the Hawking radiation process, the exponent of the Bekenstein-Hawking entropy represented the density of state, which can be written as an $(p)^{pl_P^2}$. Eq.(4.4) shows that the area of the black hole increases over time in a discrete way according to the distribution of prime numbers. In

unitary description of BH, there is an increasing in the Planck surfaces in the horizon according to the integer p . We notice that from Eq.(4.4), The information of depends not only on the geometry but also the arithmetic of coding of the unit cells.

5 Fermi–Dirac of prime number state

Next we build a unitary processes, describing the interior and near horizon the black hole vacuum states. The number of excited states that can be built is

$$N_{tot} = N_{con} = \left(1 + \frac{1}{p}\right) \times N_{vac}, \quad (5.1)$$

when $p = \infty$ we get $N_{tot} = N_{vac}$. The prime number p represents the encoding of the information on the horizon. As a result, we find the Fermi–Dirac particle-energy distribution

$$N_{vac} = \frac{N_{tot}}{e^{-\frac{S_{BH}}{ql_P^2}} + 1}. \quad (5.2)$$

If $q = 0$, we obtain $N_{vac} = N_{tot}$. We notice that N_{vac} is the two point functions of the q -modes [25]. We can immediately see that the simplest horizon corresponds to a thermal ensemble of Fermi–Dirac configuration, which justifies our focus on the number of connected components of \mathcal{F}_N . Therefore, the prime power N obtained by the Farey sequence, generates the Fermi-Dirac statistics. This implies that we can interpret $S_q = ql_P^2$ as an entropy of q cell of the horizon with the quantum microstates $|\psi_q\rangle$, where $q = 1, 2, \dots, p$ and p is the total number of black hole states.

The horizon and near horizon region are described by the microstate $|\psi_q\rangle$. The analysis described above indicates that the vacuum state is defined by $a^{(1)}|\psi_1\rangle = 0$ and $a^{(q)}|\psi_q\rangle = |\psi_{q-1}\rangle$, where $a^{(1)}$ annihilates all the vacuum states. A state in which describes the black hole can be constructed by acting $a^{(q-1)\dagger}|\psi_{q-1}\rangle = |\psi_q\rangle$, where $a^{(q)\dagger}/a^{(q)}$ are the creation/annihilation operators of order q . For $p = 2$ we obtain $N_{vac} = 2^q$. The states $|\psi_{r>n}\rangle$ corresponding to the black hole radiation by thermal ensembles of excitations with the temperatures $1/\beta$. Later, we shall see that the quantum Hall effect from this entropy. Using Eq.(5.2), we define the entropy of the code space $H_{code} \subseteq H_{CFT}$ [15] of q -cell in the horizon by

$$S_q = l_P^2 \frac{\log N_{vac}}{\log p}. \quad (5.3)$$

According to [15], we notice that $S_p \sim \log |H_{code}|$. In this case there exists a subspace $H_{code}^{(q)} \subseteq H_{code}$ of q cell (q microstates). By equivalence, we get $S_q \sim \log |H_{code}^{(q)}|$. The q cell is characterized by q -bit code [26]. So that $\log |N_{vac}|^{\frac{l_P^2}{\log p}} = \log |H_{code}^{(q)}|$. We can express the Bekenstein-Hawking entropy and the entropy of a vacuum of coding entropy

in terms of the encoding entropy S_q as $S_{vac} = S_q \log p$ and $S_{BH} = S_p \log p$. The presence of $\log p$ in the entropy S_{BH} , implies a discontinuity of the entropy at the level of the information coding.

$$S_{BH}/l_P^2 = p \times \log p \quad ; \quad S_q/l_P^2 = \log N \times \frac{1}{\log p} \quad (5.4)$$

By comparing the black hole entropy Eq.(4.4) with the coding entropy Eq.(5.3). We notice that when there is an increase in p -cell over time, there is an increasing in S_{BH} , and a decrease in S_q . Therefore, during the increase of the BH area, the encoding entropy decreases, which shows that the entropy S_q is the von Neumann entropy of the Hawking radiation [27]. Since we are studying the the black hole in AdS background, where there is the presence of time. If we assume that S_q is the von Neumann entropy of the Hawking radiation. The evolution of p -cell is proportional to time t , in this case we propose that $\mathcal{P} = \log p \sim t$.

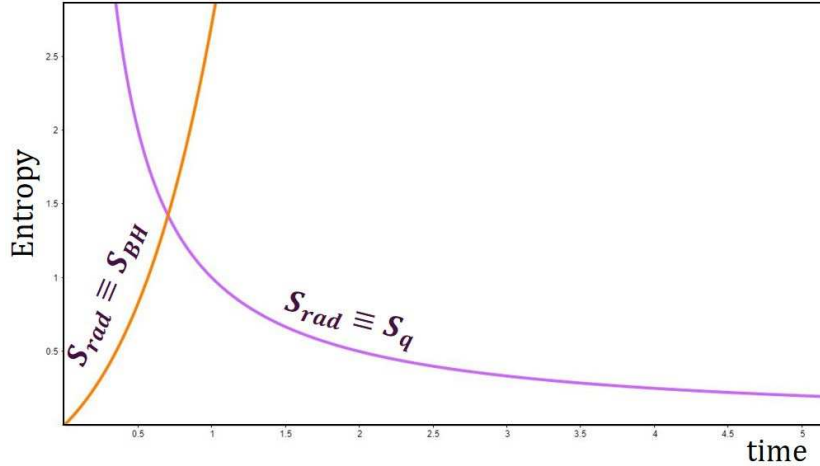


Figure 5: This figure shows the behaviors of $S_{BH}/l_P^2 = \mathcal{P}e^{\mathcal{P}}$ dashed line and $S_q/l_P^2 = \frac{\log N_{vac}}{\mathcal{P}}$ dashed line in terms of \mathcal{P} . We suppose that \mathcal{P} is continuous.

According to the Fig.5, and the two equations (5.4), the quantum state follows $\log p$ inside black hole, and they come out of the black hole in the form of radiation. Outside the black hole, they follow $1/\log p$, which changes the direction of these radiation, then they fall on the horizon. On the other hand, there is a problem, it is that the change of entropy S_{BH} (interior) to S_q (exterior), must occur in the Page time. But we see that there is a return of the radiations in the black hole to another emission, indeed there are always emissions and returns of these radiations Fig.6. To solve this problem, there are very important indications in the entropies Eq.(5.4), these entropies are discrete according to the prime number p . This shows that there is emission of radiation in an interval of time, until the first page time, then there is a return of these radiation to

the black hole according to the geodesics of the Farey diagram. When all the radiations return, it proceeds to the second emission, and the same scenario is always repeated. To see things more clearly we use some numerical values:

(1) the first emission of radiation according to $\log 2$, until the page time t_{p2} , then it returns to the black hole according to $1/\log 2$.

(2) the second emission of radiation according to $\log 3$, until the page time t_{p3} , then it returns to the black hole according to $1/\log 3$.

(3) the third emission of radiation according to $\log 5$, until the page time t_{p5} , then it returns to the black hole according to $1/\log 5$.

⋮

(p) the p -th emission of radiation according to $\log p$, until the prime page time t_{pp} , then it returns to the black hole according to $1/\log p$.

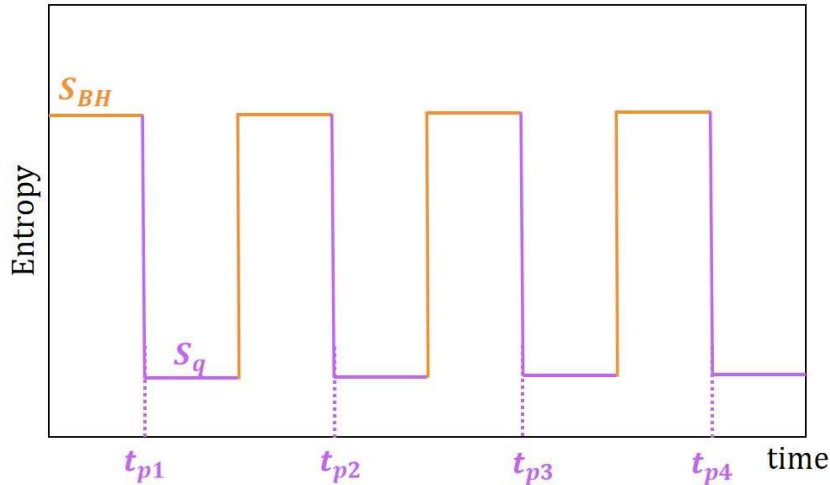


Figure 6: This figure shows the periodicity of emission and return of Hawking radiation in the case of an isolated black hole, which is equivalent to generalized Page curve.

The emission of the Hawking radiations occurs in a discrete time $t \sim \log p$ and are returned is done in the reverse of this discrete time. When Hawking radiation falls on the horizon, he will have the production of a resistance which resists radiation from entering the black hole. For that we will study in the next section the type of this resistance and its influence in this radiations.

6 Quantum Hall effect in the horizon

To explain the quantification of the entropy values and the other physical properties in this model, we propose to study the the Hall resistance in the black hole. Because we

know that in the quantum Hall models, the values of the Hall resistance are quantified. Also because we have already seen in Fig.3 that there is the presence of the semi-circles in the edge of Farey diagram, which indicates the edge states. Using the black hole first law of thermodynamics for semiclassical black holes reads $S_{BH} = \int dM/T = A/4$. One could also choose $S_p \equiv \int dM/T_p$. In the simple case, we define the resistance R_H which depends on the temperature of p cell as

$$R_H(q) = \frac{4\pi\epsilon_0 k_B T_p \log p}{c^3 M} \equiv \frac{T_p \log p}{M}, \quad (6.1)$$

or equivalently

$$R_H(p) = \frac{1}{l_P^2 p}. \quad (6.2)$$

We notice that the expression Eq.(6.2) is exactly like with the Hall resistance R_H in the quantum Hall effect, because p is integer: $R_H = h/e^2\nu = 1/G_H$, where h is Planck's constant, e is the elementary charge and G_H is the quantized Hall conductivity. The number ν can take on either integer ($\nu = 1, 2, 3, \dots$) or fractional ($\nu = (1/3, 2/5, 3/7, \dots)$). It is a simple consequence of the motion of charged particles in the near horizon region. In this case the entropy Eq.(5.3) represent the quantized Hall conductivity [28], i.e. l_P is the elementary area of the elementary charge e . The most important remark is when the number of p cells is infinite, the resistance R_H is zero, then there is no more evaporation of the black hole ($T_\infty = 0$).

From Eqs.(5.3,6.1,6.2) we get

$$S_p \equiv G_H \propto \frac{1}{T_p}. \quad (6.3)$$

This last relation is similar to **Wiedemann-Franz law** [29], i.e. the electrical conductivity of metals at normal temperatures is inversely proportional to the temperature. Also we have $R_H(p) = 1/S_{BH} \sim 1/A$, which checks the law of the **Pouillet's law** [25]. Recall that the quantum Hall is observed in two-dimensional electron systems. This result corresponds exactly with area law, which connects the entropy of black hole with the surface of horizon. We notice that the relation between area law and the entropy S_q , is described by the relation Eq.(5.2). The electrical resistance in the Pouillet's law can be expressed as

$$R_H = \frac{r}{A\sigma}, \quad (6.4)$$

where A is the cross-sectional area, r is a distance between the horizon and the charged near horizon region, σ is the conductivity of the matter (material) in the near horizon region. From Eqs.(6.2,6.4), we obtain

$$A\sigma = prl_P^2. \quad (6.5)$$

If the total number of cells equal to 1; i.e. $n = A/4l_P^2 = 1$, we find $\sigma_1 = \frac{r}{4}$. If we assume that r is the thickness of the region between the black hole and the photon sphere, we can express in this case σ as $\sigma_1 = \frac{1}{4}(r_{ps} - r_H)$, where r_{ps} is the radius of the photon sphere. In this region, we have electrically charged particle interacting with electromagnetic field. Then, we propose a representation of the near horizon geometry in terms of magnetic field B . We have a creation of a magnetic field on each cell with the magnetic length l_B , which will be proportional to Planck length l_P . We can interpret this result by creating of an electric current passing through the horizon in a magnetic field.

From Fig.4 and Fig.2, we can use the quotients of the Poincaré disk [30] to construction of the wormhole spatial geometries. From Farey graph Fig.4, we notice that the circles are only the displacement of charges on the black hole surface, and the interior of the black hole behaves as a topological insulator. In a classical point of view, the charged particles move in circular motion (the cyclotron orbit) in the horizon with a uniform perpendicular magnetic field. This rotational motion predicts the existence of edge states in the the black hole horizon. This concept makes it possible to see the lines are equipotential lines.

7 Discussion

(i) *Summary.*

This paper, based on the geometrization of the near-horizon region. We noticed that there is a new geometry hiding in the TFD states. In this framework we have defined and studied new states expressed as a function of TFD state and for an infinite temperature. We have divided the horizon into two sub-regions; the left horizon \mathcal{H}_L and the right horizon \mathcal{H}_R . Our results clearly demonstrate that the connection between the two horizons \mathcal{H}_L and \mathcal{H}_R is realised by the Möbius function. The evolution of the TFD state in the horizon allows to distinguish between two cases of the number of particles $\{N = 1, N \succ 1\}$. We have geometrized the near horizon region by the Farey diagram \mathcal{F}_N . The use of the number of connected components of \mathcal{F}_N , leads to describe unitary cells of the horizon. This description is done by the Fermi–Dirac distribution. From this distribution, we have demonstrate the existence of cells that contain quantum information. The number of connected components in Farey diagram encode the quantum information in cells. The q cell is characterized by q -bit code and the prime number of states p . Each q cell is described by the entropy $S_q = ql_P^2$ and the quantum microstates $|\psi_q\rangle$. If q equals the total number p (prime number) of cells in the horizon, the Bekenstein-Hawking entropy will be equal to $pl_P^2 \log p$. Following this procedure, we have write the Bekenstein-Hawking entropy in logarithmic term. We have found the expression of the horizon resistance in terms of $1/p$ and which is exactly similar to the

Hall resistance R_H in the quantum Hall effect. The formulation of this resistance leads to a new description of the black hole evaporation. *As a brief summary*, we have used the relationship between geometry and number theory to describe the encoding of quantum information on the horizon and black hole evaporation, which shows us that the black hole behaves like a topological insulator. The geometry of CFT states, is represented by the Farey diagram, behind this diagram it has a physics description, this is a unitary description of quantum Hall effect in the Fermi–Dirac statistics.

(ii) *Radiation journey.*

During the increase of the black hole entropy according to the quantum information of the CFT states, there is a production of the traces of information in AdS background. This connection intrinsic connection between geometry and information is already known in holographic principle [32, 33]. The traces of the information in AdS geometry are described by the geodesics and the lines of the Farey diagram. After the first Page time, there is the beginning of the radiations emission. This radiations follow the geodesic of AdS- Farey diagram then they fall in the horizon. During the transfer of radiation to information inside the black hole, the horizon resists the passage according to quantum Hall effect, this scenario always repeats. The increase of the black hole entropy implies the increase of the geodesic circles of the radiation in the exterior region. This geodesic of the exterior region represents the bath coupled to the AdS black hole. If the black hole is not isolated, and it still absorbs matter and energy, its area increases also and the Farey geodesic region also increases. In this case, the radiation travel through a long path before they return to the black hole.

References

- [1] Hawking, S. W. (1976). *Breakdown of predictability in gravitational collapse*. *Phys. Rev. D*, 14(10), 2460.
- [2] Maldacena, J. (1999). *The large- N limit of superconformal field theories and supergravity*. *International journal of theoretical physics*, 38(4), 1113-1133.
- [3] Unruh, W. G., & Wald, R. M. (2017). *Information loss*, *Rep. Prog. Phys.*, 80(9), 092002.
- [4] Page, D. N. (1993). *Information in black hole radiation*, *Phys. Rev. Lett.* 71(23), 3743.

- [5] Gautason, F. F., Schneiderbauer, L., Sybesma, W., & Thorlacius, L. (2020). *Page curve for an evaporating black hole*, *J. High Energy Phys.*, 2020(5).
- [6] Chen, Y. (2020). *Pulling out the island with modular flow*, *J. High Energy Phys.*, 2020(3), 1-21.
- [7] Almheiri, A., Engelhardt, N., Marolf, D., & Maxfield, H. (2019). *The entropy of bulk quantum fields and the entanglement wedge of an evaporating black hole*, *J. High Energy Phys.*, 2019(12), 1-47.
- [8] Ryu, S., & Takayanagi, T. (2006), *Holographic derivation of entanglement entropy from the anti-de sitter space/conformal field theory correspondence*, *Phys. Rev. Lett.*, 96(18), 181602.
- [9] Freedman, M., & Headrick, M. (2017), *Bit threads and holographic entanglement*. *Communications in Mathematical Physics*, 352(1), 407-438.
- [10] Guo, G., Wang, P., Wu, H., & Yang, H. (2021). *Scalarized Einstein-Maxwell-scalar Black Holes in Anti-de Sitter Spacetime*. *arXiv preprint arXiv: 2102.04015*.
- [11] Maldacena, J., & Susskind, L. (2013), *Cool horizons for entangled black holes*, *Fortschritte der Phys.*, 61(9), 781-811.
- [12] Balasubramanian, V., Kar, A., Parrikar, O., Sárosi, G., & Ugajin, T. (2021). *Geometric secret sharing in a model of Hawking radiation*, *J. High Energy Phys*, 2021(1), 1-44.
- [13] Bao, N., Chatwin-Davies, A., Pollack, J., & Remmen, G. N. (2019). *Towards a bit threads derivation of holographic entanglement of purification*. *J. High Energy Phys*, 2019(7), 1-24.
- [14] Akal, I., Kusuki, Y., Shiba, N., Takayanagi, T., & Wei, Z. (2021). *Entanglement Entropy in a Holographic Moving Mirror and the Page Curve*, *Phys. Rev. Lett.*, 126(6), 061604.
- [15] Penington, G. (2020), *Entanglement wedge reconstruction and the information paradox*, *J. High Energy Phys.*, 2020(9), 1-84.
- [16] Remmen, G. N., Bao, N., & Pollack, J. (2016), *Entanglement conservation, ER=EPR, and a new classical area theorem for wormholes*, *J. High Energy Phys*, 2016(7), 1-15.

- [17] Dai, D. C., Minic, D., Stojkovic, D., & Fu, C. (2020), *Testing the ER= EPR conjecture*, *Phys. Rev. D*, 102(6), 066004.
- [18] Maldacena, J. (2003). *Eternal black holes in anti-de Sitter*. *J. High Energy Phys.*, 2003(04), 021.
- [19] Verlinde, H. (2020), *ER= EPR revisited: on the entropy of an Einstein-Rosen bridge*, *arXiv preprint arXiv: 2003.13117*.
- [20] Pascoli, Silvia, and Jessica Turner (2020), *Matter–antimatter symmetry violated*, *Nature*, 323-324.
- [21] Gharibyan, H., & Penna, R. F. (2014), *Are entangled particles connected by wormholes? Evidence for the ER= EPR conjecture from entropy inequalities*, *Phys. Rev. D*, 89(6), 066001.
- [22] Mukherjee, A., Mukhi, S., & Nigam, R. (2007). *Dyon death eaters*. *J. High Energy Phys*, 2007(10), 037.
- [23] Gaster, J., Lopez, M., Rexer, E., Riell, Z., & Xiao, Y. (2020). *Combinatorics of k -Farey graphs*. *Rocky Mt J Math*, 50(1), 135-151.
- [24] Nomura, Y., & Weinberg, S. J. (2014). *Entropy of a vacuum: What does the covariant entropy count?*. *Phys. Rev. D*, 90(10), 104003.
- [25] Zyul'kov, I., Armini, S., Opsomer, K., Detavernier, C., & De Gendt, S. (2019). *Selective electroless deposition of cobalt using amino-terminated SAMs*. *J. Mater. Chem. C*, 7(15), 4392-4402.
- [26] Hayden, P., & Penington, G. (2020). *Approximate quantum error correction revisited: introducing the alpha-bit*. *Commun. Math. Phys.*, 374(2), 369-432.
- [27] Buoninfante, L., Di Filippo, F., & Mukohyama, S. (2021). *On the assumptions leading to the information loss paradox*, *J. High Energy Phys.*, 2021(10), 1-26.
- [28] Hasan, M. Z., & Kane, C. L. (2010). *Colloquium: topological insulators*. *Rev. Mod. Phys.*, 82(4), 3045.
- [29] Kubala, B., König, J., & Pekola, J. (2008). *Violation of the Wiedemann-Franz law in a single-electron transistor*. *Phys. Rev. Lett.*, 100(6), 066801.
- [30] Akers, C., Engelhardt, N., & Harlow, D. (2020). *Simple holographic models of black hole evaporation*. *J. High Energy Phys.*, 2020(8), 1-14.

- [31] Krasnov, K. (2000). *Holography and Riemann surfaces*. arXiv preprint, hep-th/0005106.
- [32] Hooft, G. T. (1993). *Dimensional reduction in quantum gravity*. arXiv preprint gr-qc/9310026.
- [33] Susskind, L. (1995). *The world as a hologram*, *J. Math. Phys.* 36(11), 6377-6396.
- [34] Li, H., & Li, T. (2018). *Recursive sequences in the Ford sphere packing*, *Chaos Solit. Fractals*. 106, 94-106.